Title

Role of underlying surface, rainstorm and antecedent wetness condition on flood responses in small and medium sized watersheds in the Yangtze River Delta region, China

Authors
Wang, Qiang
Xu, Youpeng
Cai, Xitian
et al.

Publication Date
2021-11-01

DOI
10.1016/j.catena.2021.105489

Role of underlying surface, rainstorm and antecedent wetness condition on flood responses in small and medium sized watersheds in the Yangtze River Delta region, China

Qiang Wang [a, c], Youpeng Xu [a,*1], Xitian Cai [b, c], Jinyun Tang [c], Long Yang [a]

[a] School of Geography and Ocean Science, Nanjing University, Nanjing, China

[b] School of Civil Engineering, Sun Yat-sen University, Guangzhou, China

[c] Climate and Ecosystem Sciences Division, Lawrence Berkeley National Laboratory, Berkeley, CA, USA

[1]Corresponding author at: No. 163 Xianlin Avenue, Nanjing, Jiangsu Province, P.R.China.

E-mail address: xypnju@163.com (Y. Xu)

Abstract

Floods are becoming more frequent and are hard to control due to the shortage of water conservancy projects in small and medium sized basins, especially in developing regions. Understanding the hydrologic responses and estimated flood characteristics to storm events can help to predict flood disasters and form better effective mitigation and adaptation strategies. Using observations of several representative watersheds and Artificial Neural Networks (ANN) and Principal Component Regression (PCR) models, we conduct data-driven analyses to examine the flood responding characteristics. We quantified the relative contributions of the influencing factors to the variation of each flood characteristic. Statistical analysis of the observations shows that the drainage area plays a key role in determining the distribution of lag time and peak discharge. Rainstorm variability has direct influence on floods, and typhoon-induced rainstorms with high total rainfall and rainfall intensity generate higher lag time, flood peak, unit discharge and runoff depth, but lower runoff coefficient. The ANN and PCR models accurately predicted the variations of flood features using the driving factors including physical geographical characteristics, rainstorm features, and antecedent condition. Physical geographical characteristics. Physical geographic characteristics are key influential factors of lag time, flood peak and runoff coefficient, while the rainstorm features control the magnitude of unit discharge and runoff depth. These results indicate that floods are mainly affected by rainstorm features and physical geographic characteristics in the Yangtze River delta, and it might become more damaging with the increasing rainfall extremes and sprawling impervious surfaces in a changing environment.

Keywords: Flood response; Data-driven analysis; Small and medium sized basins; the Yangtze River Delta

1. Introduction

Floods, triggered by rainstorms, often cause huge losses of human life and property. Unfortunately, they have been observed to become more frequent and intensive over past few decades due to climate change and anthropogenic activities (Blöschl et al., 2019; IPCC, 2013; Y Winsemius et al., 2016; in et al., 2018). Especially in small and medium sized watersheds (with areas usually smaller than 2500 km^2), liquid floods, debris floods or debris flows occur quickly and are hard to forecast, leading to huge destruction (Silvestro et al., 2011). However, it is difficult to reduce the flood disaster through hydraulic scheduling measures, due to the shortage of water conservancy projects such as lock, dam, and reservoir in these watersheds, especially in the developing regions. Thus, understanding the hydrologic responses and estimated flood characteristics to storm events in small and medium sized basins are prerequisites for prediction of flood disasters (Borga et al., 2014), so that the society can form better effective mitigation and adaptation strategies.

Previous studies have investigated the relationship between influential factors, such as rainfall, drainage area, antecedent wetness, and urbanization, with flood responses (Bennett et al., 2018; Borga et al., 2008; Song et al., 2019; Yang et al., 2016; Zhou et al., 2017; Blöschl et al., 2019). However, difficulties remain in attributing specific changes in floods to specific watershed characteristics due to the limited spatial coverage and number of gauging basins. Especially in developing regions, such as the Yangtze River Delta, flood disasters are becoming more and more severe with rapid underlying surface changes during the development of urbanization, and understanding its consequence is becoming more imperative.

Urbanization, characterized by replacing permeable vegetated land surface with impervious surface areas, would significantly change the regional water cycle processes (Wang et al., 2018; Zhou et al., 2013). However, due to the complexities of urban floods, detected responses might differ among regions (Wang et al., 2018; Woldesenbet et al., 2016; Yan et al., 2013; Zhou et al., 2017), and quantifying the impacts of impervious surface on floods is still fraught with difficulties. Moreover, existing impacts assessment studies often analyzed a single basin, which fail to account for the potentially substantial combined impacts of the heterogenous and multi-scale nature of basin properties (Zhou et al., 2017).

However, the relative contributions of potential influencing factors on floods are still not clear thanks to the complexities of flood response. Hydrological experimentation and observations are basic approaches to understand the key mechanisms of water resources systems (Bosch & Hewlett, 1982; Hopmans & Pasternack, 2006; and Tang et al., 2016). Experiment observations can help evaluate hydrologic model simulations and quantify their uncertainties due to model deficiency. With the multi-disciplinary development of science and technology, many hydrological experimental basins have been built across the world, which help to understand the mechanism of flood response under changing environment. However, relatively few hydrologic observation experiments have conducted in rapid developing region focusing on the problem of floods. This is especially true for floods occurring in small and medium basins, because they develop at various space and time scales and monitoring them requires data of high temporal and spatial resolution (Borga et al., 2008). The Yangtze River Delta region is one of the most populous and economically developed areas in China, and is prone to flood disasters due to Mei-yu frontal rainfall and tropical cyclones, e.g., typhoon, thus hydrological observations with high temporal and spatial resolution are critical.

In the Yangtze River Delta region, the gauging stations are scarce and the underlying surfaces have experienced dramatic changes through the urbanization during the past few decades. Exploring the response mechanism of floods can provide important scientific support for flood control and disaster reduction in this region. Due to the scarcity of gauging watersheds and the importance for understanding flood responses, we here selected and continuously observed nine representative watersheds located in the Yangtze River Delta region, ranging in drainage area from 1.6 to 2798.9 km^2. Observations from these watersheds are selected to investigate the flood responses in watersheds differ in drainage areas, impervious surface coverage, and topography. We examined changes in flood characteristics with the variations of land surface properties, rainstorm characteristics and antecedent conditions.

The objective of this study is to detect the critical factors influencing flood characteristics and quantify the contribution its relative contributions in small and medium scale watersheds. And this objective is resolved by addressing the following questions: (1) How do the distributions of lag time and peak flow vary with watersheds' main physiographic characteristics? (2) What are the dominant factors determining the flood peaks and rainfall-runoff relationships? (3) What are the relative contributions of each influencing factor on flood characteristics? The data-driven answers based on hydrologic observations will undoubtedly contribute to complementing our limited understanding of flood generation mechanisms in a changing environment, and help to regional prevention and control of flood disasters.

2. Materials and Methods

2.1 Study Area

The Yangtze River Delta region, located in eastern China, covers an area of 95,400 km^2 (Figure 1). The climate of the region is dominated by the East Asia monsoon, with annual temperature and precipitation ranging from 14 °C to 18 °C and from 1,000 mm to 1,400 mm, respectively. Influenced by East Asian monsoon, floods mainly occur from April to October caused by Mei-yu and tropical cyclones, such as typhoon, in the Yangtze River Delta. According to the type of weather system, the flood season in this region can also be broadly divided into Mei-yu (at roughly May-July) and typhoon (July-October) periods.

This region has experienced rapid urbanization since the 1980s and become one of the most populous and prosperous regions in China. Due to land cover change caused by urbanization, as well as the specific climate conditions of this area, the regional floods are becoming more serious and threatening (Zhou et al., 2013; Wang et al., 2016). In response to this situation, nine representative watersheds were selected to monitor and detect the flood response to land surface properties, rainstorm characteristics and antecedent watershed conditions, which are expected to help better understand and implement flood control and disaster reduction in the region (Table 1, Figure 1).

These basins exhibit different physical geographic features, such as spatial scale and urbanization level. Following the fraction of impervious area, these basins can be categorized as high (impervious rate >30%), medium (impervious rate is between 6%-30%) and low (impervious rate<6%) urbanized regions. In addition, according to drainage area, these basins can be recognized as medium (drainage area between 350 km^2 -2500 km^2) and small (drainage area <350 km^2) watershed.

The Shuangqiao Catchment (SQC, 1.6 km^2), located in the center of Changzhou City, is a small urban catchment with high urbanization level with 93.41% impervious rate. Hualong Creek (HLC, with area of 9.4 km^2 and impervious rate of 0.13%) and Zhongtianshe River Basin (ZTS, with area of 40.0 km^2 and impervious rate of 0.63%), Yinjiang-Jiaokou River Basin (YJR, with area of 88.0 km^2 and impervious rate of 3.95%, respectively) are small headwater watershed with low impervious area, and Luoyang River Basin (LYR, with area of 149.4 km^2 and impervious rate of 9.63%) and Nantiaoxi Basin (NTX, with area of 240.7 km^2 and impervious rate of 0.76%) are small scale watershed with medium urbanization level (Wang et al., 2019). The other three medium basins, i.e., Xitiaoxi River (XTX, with area and impervious rate of 1191.5 km^2 and 7.98%, respectively), Dongtiaoxi River Basin (DTX, with area and impervious rate of 1489.1 km^2 and 8.48%, respectively), and Qianhancun Basin (QHC, with area and impervious rate of 2106.7 km^2 and 14.82%, respectively), experienced a rapid urbanization process in the past few decades.

The land use maps show that these watersheds have different spatial characteristics, as shown in Figure 1 and Figure 2. SQC is a small yet highly urbanized catchment and its main land use type is urban land, accounting for more than 70%. HLC and ZTS are two natural watersheds with little human interference and the main land use type is forest-grass land, with 89.38% and 59.74%, respectively. YJR, NTX, XTX and DTX have experienced a rapid urbanization with fast urban expansion, but the forest-grass land remains the main land use type (more than 60%). The other two basins, LYR and QHC are moderately disturbed by humans with relatively strong agricultural activities, and their main land use type is agricultural land with the portion of 46.2% and 73.53%, respectively.

2.2 Instrumentation and Data

We have selected and observed 9 representative watersheds in the Yangtze River Delta region. The discharge station in the outlets and several rainfall gauges for each basin were set to observe streamflow and rainfall, respectively (Table 2). Here we only report the effects of rainfall temporal variability using data from automatic high-resolution monitoring rain gauges, while no spatial variability is available due to the difficulty of applying weather radar to observe multi-basin areas with complex terrain.

The number of rainfall and discharge stations for these basins are shown in Table 2. All rainfall stations and discharge stations for small basins, such as SQC, HLC, ZTS, YJR, LYR and NTX, were automatically collecting observations every 5 minutes, while other discharge stations for bigger basins are observed with hourly intervals which could monitor floods effectively in practice. And the total rainfall for each basin is estimated via the Thiessen polygon method. The hydrological observations were mainly conducted from 2013 to 2018, while some historical flood records for some bigger basins, such as XTX and QHC, are available and thus the observation periods are longer. Overall, a total of 240 storm hydrographs (rainfall for 24-h are higher than 25 mm or 12 h higher than 15 mm) with matching rainfall records during the rainy season is observed with high temporal resolution.

The land use and land cover maps in the studied watersheds for the year of the flood occurring were derived from Google and Landsat images. The land use maps of SQC, HLC, ZTS, and YJR, were obtained by digitizing Google maps due to small area, and the maps for other relative larger basins, i.e., LYR, NTX, XTX, DTX, and QHC, were extracted from Landsat image using methods of supervised classification and manual interpretation with an acceptable precision. The annual impervious rate in each watershed were calculated based on the global artificial impervious area (GAIA) between 1985 and 2018 (Gong et al., 2019).

2.3 Methods

We first implemented power-law relationship, Pearson correlation coefficient and linear trend to examine the relationships between the influential factors and the flood characteristics. We selected flood lag time (the time difference between the rainfall time centroid and the time of peak discharge), flood peak, unit flood peak discharge (flood peak divided by drainage area), runoff depth (surface runoff volume divided by drainage area), runoff coefficient (runoff depth divided by total rainfall) as flood characteristics. The surface runoff was separated from streamflow using the recursive digital filter technique proposed by Lyne and Hollick (1979). These flood characteristics are all derived or calculated from observed flood events.

Potentially, basin scale, rainstorm, impervious surface area and antecedent wetness, all influence flood responses (Yang et al., 2016; Borga et al., 2014; Zhou et al., 2017). Thus, the potential influential factors of flood characteristics selected in the study consist mainly of three types of characteristics: physical geographical characteristics, such as drainage area (km^2), impervious area rate, land use intensity, river length (km), river density (km/km^2) and average slope; rainstorm (total rainfall, average rainfall intensity and maximum 1-h rainfall); and antecedent moisture conditions (initial discharge and antecedent wetness). Here the land use intensity represents a comprehensive index of land use intensification degree (Zhuang and Liu, 1997), which can be calculated as follows:

$$La = 100 \times \sum_{i=1}^{n} A_i \times C_i \quad (1)$$

where La is the land-use intensification degree in each watershed and its value varies from 100 to 400; A_i is the grading index of each land-use type, and its values for forest-grass land, agriculture land, urban land and water bodies are 1, 2, 3 and 4, respectively; and C_i is the percentage of each land-use types in each watershed (Wang et al., 2018). The average slope is presented by average percent rise of slope, which reflects the topographic feature of each basin and is calculated using 30-m resolution Digital Elevation Model (DEM) in ArcGIS 10.3.

To detect the effects of weather systems on floods, we associate an annual flood event of a given basin with a tropical cyclone by following the algorithm, i.e., if the center of a tropical cyclone is within 500 km of the basin during a time window of 72 h centered on the occurrence time of the flood peak (Yang at al., 2019). Allowing the weather systems, we divided observed 240 flood events into typhoon-induced floods (59 events) and other (without typhoon-induced) floods (181 events).

The Artificial Neural Networks (ANN) and Principal Component Regression (PCR) were used to estimate the flood characteristics based on the influential factors and quantify the relative contributions of each influential factor. Fully connected machine learning algorithm (neural networks) was used to predict flood response and quantify the relative contributions of each flood influential factor. ANN algorithm is a function of a set of derived inputs called hidden nodes, which are nonlinear functions of the original inputs (potential influential factors). ANN has been widely to detect the response of nonlinear relationships in the hydrological system (see, e.g., Chen & Chang, 2009; Dawson & Wilby, 2001). We used half of the observed data as training set randomly, the retained half for validation. The best number of hidden nodes is determined by the model with best performance for training data. The relative contribution of each input (potential influential factors) to outputs (flood characteristics) is quantified by the Garson's algorithm based on weight matrix (Garson, 1991). In addition, due to the potential multicollinearity of these input variables, the multiple linear regression cannot be used directly. Thus, PCR were also applied to estimate the flood characteristics using the relative influential factors, and then the relative importance of the principal components of each type of characteristics were quantified (Grömping, 2006)

3. Results and Discussion

3.1 Flood Response to Physiographic Characteristics

Lag time and peak discharge are two main characteristics of flood and highly relevant to flood prewarning time and destructiveness. We examined the responses of lag time and peak discharge to the basin scale (Figure 3 and Figure 4). As shown in Figure 3, drainage area plays a key role in determining the distribution of flood lag time for these observed watersheds. As drainage area increases, the lag time of flood usually increases. However, Figure 3 also illustrates that basin scale is not the only factor that affects flood lag time. For instance, the lag time for LYR and XTX is almost the same despite the former basin has a much smaller area, perhaps due to the less steep slope for LYR.

The distribution of flood lag time in this study are similar to the findings of Borga et al. (2014) and Creutin et al. (2013), as the envelope red lines and equations shown in Figure 3. Most of the lag times of floods are enveloped by limit response time. The bottom limit line for basins with small scale (<350 km^2) has gentle slope and the distributions were getting further away from the envelope dotted red lines, which indicates that the flood lag time in smaller basins is more susceptible to other factors. The results also show that, flood lag times might shorten or increase in certain flood events, especially in small catchments with high human intervention, such as SQC.

We next fit the power-law relationship to the envelope curves that relate the lower and upper limits of flood peak (i.e., P_L *and* P_U (h)) to watershed area A (km^2). These relationships are as follows:

$$P_L = 0.1 \times A^{0.9} \quad (2)$$

$$P_U = 6 \times A^{0.9} \quad (3)$$

Figure 4.a shows the distributions of flood peak exhibit large variation across different watersheds, and all the flood peaks fall in the envelope of lower and upper limits. The flood peak increases with the basin scale, with less influences from other factors. For instance, SQC and LYR, with relative higher urbanization level and smaller spatial scale, would generate big magnitude of peak discharge with HLC and NTX, respectively, indicating the impervious surface rate is also influential. In addition, the flood peak distribution in XTX is higher than DTX and QHC, basins with greater area but gentle slope. The pattern of distribution for unit discharge is shown in Figure 4.b, which illustrates that the basin with high impervious surface rate (SQC) and steeper slope (such as YJR and XTX) would produce higher peak discharge for unit area.

The distribution of lag time and peak discharge for floods showed that the basin scale is a main influential factor affecting the magnitude of floods, meanwhile, watershed topography and impervious surface features also play important roles. Further analyses are needed to refine the quantification of contributions of each specific factor.

3.2 Flood response to rainstorm characteristics

3.2.1 Impacts of rainstorm characteristics

Extreme rainstorms directly trigger floods. The total rainfall, average rainfall intensity and maximum 1-h rainfall are used to characterize the rainstorms. We calculated the Pearson correlation coefficient (*R*) between each flood characteristic (flood peak, unit discharge, runoff depth, and runoff coefficient) and each rainstorm feature to preliminarily explore the relationship between influencing factors and flood characteristics (Table 3).

Flood peak, unit discharge and runoff depth in most basins have high positive correlation with three rainstorm characteristics, which indicates that rainstorm is the main cause of flood in the Yangtze River Delta region. The region is characterized by summer subtropical monsoon, thus precipitation mainly contributed to the hydrological responses (Song et al., 2019). Specifically, for the smallest urban catchment (SQC), the impacts of average rainfall intensity and maximum 1-h rainfall on flood peak and unit discharge are higher than the impacts of total rainfall, while opposite impacts are found for other larger basins. With respect to runoff depth, it is strongly correlated with the total rainfall and the influences of total rainfall are all higher than maximum 1-h rainfall for all studied basins. However, results also show that there is no significant correlation existing between the runoff coefficient and each rainfall characteristic in most study basins, and even exists negative correlations but insignificant. This is because the influencing mechanism of runoff coefficient is more complicated, and only the rainfall characteristics perhaps are hard to reflect the its variation.

It is interesting that those basins with distinct physiographic features demonstrate similar distributions of runoff coefficient, except SQC and HLC (Figure 5). Most runoff coefficients for flood events range from 0.25 to 0.75. Controlled by East Asian summer monsoon, floods mainly occur in rainy season, and the difference of runoff coefficient is thus relatively small due to similar soil moisture situations following abundant summer rainfall. The exceptional distributions of runoff coefficient in some basins indicates the effects of land use and land cover. For examples, the urban catchment, such as SQC, have highest runoff coefficient, while HLC, another small forest catchment but with lowest impervious surface rate, has smallest runoff coefficient.

3.2.2 The impacts of weather systems

Weather systems can affect the characteristics of rainstorm, and thus influence the flood process. We examine the rainstorm and flood characteristics for each basin under typhoon and without typhoon, as shown in Figure 6 and Figure 7. The results showed that rainstorm under typhoon would generate much more total rainfall, and a little larger maximum 1-h rainfall and average rainfall intensity (Figure 6). But for the SQC, the rainstorm events caused by typhoon have higher total rainfall, but lower maximum 1-h rainfall and average rainfall intensity.

Accordingly, floods, caused by typhoon, have higher lag time, flood peak, unit discharge and runoff depth. However, there has a litter lower distribution for runoff coefficient for floods under typhoon compared with the events without typhoon. These results also indicate that lag time, flood peak, unit discharge and runoff depth mainly affected by rainstorm characteristics, while runoff coefficient are more susceptible to other factors, such as physical geographical characteristics and antecedent moisture condition. The typhoon events mainly occur in late periods of rainy season, with a relatively dry climate and lower antecedent moisture condition, which might lead to a little lower distribution of runoff coefficient.

3.3 Flood Response to Antecedent Watershed Conditions

The correlation analysis between each flood characteristic and initial discharge with antecedent wetness was also carried out to examine the flood response to antecedent watershed conditions, respectively (Table 4). Here antecedent wetness is evaluated using rainfall accumulations within a temporal window of 72 h prior to the beginning of a rainstorm.

There are no strong direct relationships found between each flood characteristic with both initial discharge and antecedent wetness for most small-scale basins (Table 4). Similarly, Garg and Mishra (2019) and Zhou et al. (2017) also reported weak effects of antecedent conditions on floods. However, some other researchers found that antecedent conditions greatly affect the process of floods on hydrological modeling (Fang & Pomeroy, 2016; Cea & Fraga, 2018). Perhaps in humid regions, the effects of antecedent conditions on short term flood process are limited. Soil moisture content in the rainy season has been maintained at a relatively high level, with relatively small changes, so its impact on the flood is relatively small, especially in forest watershed. The results indicate that the floods in basins with intense agricultural activities, such as QHC, are more likely to be affected by antecedent conditions (Table 4). Antecedent wetness mainly affects rainfall infiltration and thus the flooding processes (Cea et al., 2018; Fang et al., 2016). However, the Yangtze River Delta region is humid and controlled by the summer monsoon, the antecedent conditions have little difference during flood season and thus little impacts on floods. In addition, the observed rainstorm floods are relatively large magnitude, and thus the role of antecedent conditions decreases (Bennett et al., 2018).

3.4 The relative contributions of each influential factor on flood response

We next estimate flood responses to the physical geographical characteristics, rainstorm and antecedent moisture conditions through the ANN and PCR algorithm, and further quantify relative contributions of these influential factors on flood responses. There are 11 input variables, including physical geographic characteristics (drainage area, average slope, impervious surface coverage, land use intensity, river length and river density), rainstorm features (total rainfall, average rainfall intensity and maximum 1-h rainfall) and antecedent moisture conditions (initial discharge and antecedent wetness). Flood lag time, flood peak, unit discharge, runoff depth and runoff coefficient are separately served as output variables, respectively. All variables are normalized before constructing models.

Comparisons among actual and predicted data and the metrics of model performance for ANN and PCR are shown in Figure 8. All R values of models for lag time, flood peak, unit discharge, and runoff depth in both training and testing datasets are statistically significantly. This suggests that the models of ANN and PCR both could accurately predict the variations of lag time, flood peak, unit discharge and runoff depth using the driving factors including physical geographic characteristics, rainstorm features and antecedent moisture conditions. For runoff coefficient, we found that the ANN model can simulate its general variation trend but with a relatively larger error. From analyses in previous sections, we noticed that the runoff coefficient varies very little in the studied basins (so that observations has little information of this variable) and hence is relatively hard to predict.

Basically, the ANN and PCR model could predict the variations of flood characteristics with satisfied performance.

The relative contributions of each factor to each flood characteristic were then quantified, as shown in Figure 9. ANN has strong ability for simulating nonlinear relationship between independent variables. Thus, all potential influencing factors have been selected to detect the individual impacts on flood. However, the collinearity of independent variables should be considered when using the PCR method, thus only the relative contributions of main components were quantified. The contributions of same types factors are combined in the figure 9. The results show that the relative contributions that estimated by ANN and PCR are basically consistent, but still with some differences. And then ensemble mean values of ANN and PCR were calculated to reduce the uncertainty introduced by different model.

The results showed that the contributions of physical geographic characteristics, rainstorm and antecedent moisture conditions on flood lag time decreased in turn, and physical geographic characteristics contribute more than 50% both in ANN and PCR (Figure 9). Specifically, the ensemble means of the impacts for three type factors., i.e., physical geographic characteristics, rainstorm and antecedent moisture conditions, on lag time account for 55.06%, 34.3% and 10.65%, respectively. Similarly, the impact categories affected flood peak from the highest to the least are also physical geographic characteristics, rainstorm and antecedent moisture conditions, with the contributions of 54.38%, 26.24% and 20.21%, respectively. And the impact of land use intensity is the highest among the factors predicted by ANN model. With respect to unit discharge and runoff depth, the relative impacts in turn were rainstorm, physical geographic characteristics, and antecedent moisture conditions, and rainstorms contributed more than a half. The relative contributions of physical geographical characteristics, antecedent moisture conditions, and rainstorm on runoff coefficient account for 62.26%, 22.45% and 15.2% in ensemble mean, respectively.

The above analysis indicates that physical geographic characteristics and rainstorm features have great impacts on floods, especially the influence of the underlying surface cannot be ignored， such as land use intensity and impervious surface rate. But with rapid urbanization processes, underlying surface, such as land use and cover, changed dramatically. While land use intensity has some influence on flood characteristics, such as flood peak, lag time and runoff coefficient. Many recent works also reported that rainfall extremes are increasing at both global (Chou et al., 2013, Yin et al., 2018, IPCC, 2013) and reginal scales (Wang et al., 2016) due to climate change. The Yangtze River Delta is one of largest river deltas and metropolitan areas in the world, and was developed rapidly in the past decades (Han et al., 2015). The impervious surface has expanded and is expected to continue expanding (Gong et al., 2020), which unavoidably change the flood processes in this region. Floods might become more frequent and damaging due to increasing extreme rainstorms and land surface with dynamical changes (Winsemius et al., 2016). Hence, we suggest that disaster mitigation measures should be updated and improved to best respond to the regional floods that would likely become more severe in the years to come.

4 Conclusions

In the Yangtze River Delta region, floods occur frequently but has limited available gauging watersheds to analyze its responses. We here selected for observations in nine representative basins with different physical geographic features. We then carried out data-driven analyses of these flood events to examine the relationships between flood features (i.e., flood lag time, flood peak, unit discharge, runoff depth, and runoff coefficient) and influential factors including physical geographic characteristics (drainage area, average slope, impervious surface coverage, land use intensity, river length and river density), rainstorm features (total rainfall, average rainfall intensity and maximum 1-h rainfall) and antecedent conditions (initial discharge and antecedent wetness). A machine learning algorithm (neural networks) and PCR is then used to predict flood responses and quantify the contributions of each influential factor to these flood characteristics. We made the following main findings.

1. The power-law relationships between basin scale and floods showed that the drainage area plays a major role in determining the distribution of lag time and peak discharge of floods. As drainage area increases, the lag time and peak discharge usually increase. Meanwhile, the anomalous response in lag time in watersheds with high human intervention and flood peak in watersheds with steeper slope indicate basin slope and underlying surface characteristics are other important control factors.

2. Rainstorm variability has direct influence on floods. The Pearson correlation coefficient showed strong correlations between rainstorm characteristics, especially total rainfall, and flood features, such as, flood peak, unit discharge and runoff depth. For the smallest catchment (SQC), the impacts of rainfall intensity (average rainfall intensity and maximum 1-h rainfall) on flood peak and unit discharge are higher than the impacts of total rainfall, while opposite impact patterns are found for other basins with bigger area. For the responses of runoff depth, the influences of total rainfall are higher than rainfall intensity. In addition, rainstorms with different characteristics caused by different weather systems would have different flood

responding. Typhoon-induced rainstorms with higher total rainfall and rainfall intensity would produce high lag time, flood peak, unit discharge and runoff depth, but have a little low in runoff coefficient.

3. The relationships between flood characteristics and antecedent conditions (initial discharge and antecedent wetness) showed the antecedent conditions impacts on most basins are weak.
4. The ANN and PCR models built in this study could accurately predict the variations of lag time, flood peak, unit discharge, runoff depth, and runoff coefficient using the driving factors of physical geographic characteristics, rainstorm, and antecedent moisture condition.
5. The contributions of physical geographic characteristics, rainstorm and antecedent moisture conditions on lag time and flood peak decreased in turn, and the impact affected unit discharge and runoff depth from the highest to the least are rainstorm, physical geographic characteristics, and antecedent moisture conditions. In addition, the relative contributions of physical geographical characteristics, antecedent moisture conditions, and rainstorm on runoff coefficient account for 62.26%, 22.45% and 15.2%.

The preceding conclusions indicate that rainstorm characteristics and physical geographic characteristics have great impacts on floods. Unfortunately, recent studies have reported increasing rainfall extremes in both global (Chou et al., 2013; IPCC, 2013; Yin et al., 2018) and regional scale (Wang et al., 2016) due to climate change and the increasing impervious surface coverage (Gong et al., 2020), thus floods might become more frequent and damaging, which calls for updated and improved disaster mitigation measures in the Yangtze River Delta region, or similar developing areas with rapid urbanization.

Acknowledgments

This study was supported by the National Key Research and Development Program of China (No. 2018YFC1508201) and National Natural Science Foundation of China (No. 41771032). J.Y. Tang and X.T. Cai are supported by the Director, Office of Science, Office of Biological and Environmental Research of the US Department of Energy under contract No. DE-AC02-05CH11231 as part of RUBISCO project under the Regional and Global Climate Modeling (RGCM) Program.

References

Bennett, B., Leonard, M., Deng, Y., & Westra, S. (2018). An empirical investigation into the effect of antecedent precipitation on flood volume. Journal of hydrology, 567, 435-445. https://doi.org/10.1016/j.jhydrol.2018.10.025.

Blöschl, G., Hall, J., Viglione, A., Perdigão, R.A., Parajka, J., Merz, B., et al. (2019). Changing climate both increases and decreases European river floods. *Nature*, 573(7772), 108-111. https://doi.org/10.1038/s41586-019-1495-6.

Borga, M., Gaume, E., & Marchi, L. (2008). Surveying flash floods: gauging the ungauged extremes. *Hydrological Processes*, 22(18), 3,883-3,885. https://doi.org/10.1002/hyp.7111.

Borga, M., Stoffel, M., Marchi, L., Marra, F., & Jakob, M. (2014). Hydrogeomorphic response to extreme rainfall in headwater systems: Flash floods and debris flows. *Journal of Hydrology*, 518, 194-205. https://doi.org/10.1016/j.jhydrol.2014.05.022.

Bosch, J. M., & Hewlett, J. D. (1982). A review of catchment experiments to determine the effect of vegetation changes on water yield and evapotranspiration. *Journal of Hydrology*, 55(1), 3-23. https://doi.org/10.1016/0022-1694(82)90117-2.

Bosshard, T., Carambia, M., Goergen, K., Kotlarski, S., Krahe, P., Zappa, M., et al. (2013). Quantifying uncertainty sources in an ensemble of hydrological climate-impact projections. *Water Resources Research*, 49(3), 1,523-1,536. https://doi.org/10.1029/2011WR011533.

Cai, X., Riley, W. J., Zhu, Q., Tang, J., Zeng, Z., Bisht, G., & Randerson, J. T. (2019). Improving Representation of Deforestation Effects on Evapotranspiration in the E3SM Land Model. *Journal of Advances in Modeling Earth Systems*, 11(8), 2,412-2,427. https://doi.org/10.1029/2018MS001551.

Carvalho-Santos, C., Nunes, J. P., Monteiro, A. T., Hein, L., & Honrado, J. P. (2016). Assessing the effects of land cover and future climate conditions on the provision of hydrological services in a medium-sized watershed of Portugal. *Hydrological Processes*, 30(5), 720-738. https://doi.org/10.1002/hyp.10621.

Cea, L., & Fraga, I. (2018). Incorporating Antecedent Moisture Conditions and Intraevent Variability of Rainfall on Flood Frequency Analysis in Poorly Gauged Basins. *Water Resources Research*, 54(11), 8,774-8,791. https://doi.org/10.1029/2018WR023194.

Chen, Y., Xu, C., Chen, X., Xu, Y., Yin, Y., Gao, L., et al. (2019). Uncertainty in simulation of land-use change impacts on catchment runoff with multi-timescales based on the comparison of the HSPF and SWAT models. *Journal of Hydrology*, 573, 486-500. https://doi.org/10.1016/j.jhydrol.2019.03.091.

Chen, Y. H., & Chang, F. J. (2009). Evolutionary artificial neural networks for hydrological systems forecasting. *Journal of Hydrology*, 367(1-2), 125-137. https://doi.org/10.1016/j.jhydrol.2009.01.009.

Chou, C., Chiang, J. C. H., Lan, C. W., Chung, C. H., Liao, Y. C., et al. (2013). Increase in the range between wet and dry season precipitation. *Nature Geoscience*, 6(4), 263-267. https://doi.org/10.1038/ngeo1744.

Creutin, J. D., Borga, M., Gruntfest, E., Lutoff, C., Zoccatelli, D., & Ruin, I. (2013). A space and time framework for *analyzing* human anticipation of flash floods. *Journal of Hydrology*, 482, 14-24. https://doi.org/10.1016/j.jhydrol.2012.11.009.

Dawson, C. W., & Wilby, R. L. (2001). Hydrological modelling using artificial neural networks. *Progress in physical Geography*, 25(1), 80-108. https://doi.org/10.1177/030913330102500104.

Fang, X., & Pomeroy, J. W. (2016). Impact of antecedent conditions on simulations of a flood in a mountain headwater basin. *Hydrological Processes*, 30(16), 2,754-2,772. https://doi.org/10.1002/hyp.10910.

Garg, S., & V. Mishra (2019). Role of extreme precipitation and initial hydrologic conditions on floods in Godavari river basin, India. *Water Resources Research*, 55(11), 9,191-9,210. https://doi.org/10.1029/2019WR025863.

Garson, D. G. (1991). Interpreting neural network connection weights. *AI Expert*, 6(4), 46-51. Doi: 10.5555/129449.129452.

Gong, P., Li, X., Wang, J., Bai, Y., Chen, B., Hu, T., et al. (2020). Annual maps of global artificial impervious area (GAIA) between 1985 and 2018. *Remote Sensing of Environment*, 236, 111510. https://doi.org/10.1016/j.rse.2019.111510.

Grömping U. Relative importance for linear regression in R: the package relaimpo [J]. Journal of statistical software, 2006, 17(1): 1-27.

Han, L., Xu, Y., Yang, L. & Deng, X. (2015). Changing structure of precipitation evolution during 1957–2013 in Yangtze River Delta, China. *Stochastic Environmental Research & Risk Assessment*, 29(8), 2,201-2,212. https://doi.org/10.1007/s00477-015-1034-4.

Hopmans, J. W., & Pasternack, G. (2006). Experimental hydrology: A bright future. *Advances in Water Resources*, 29(2), 117-120. https://doi.org/10.1016/j.advwatres.2005.04.016.

Lyne, V., Hollick, M. (1979, September). Stochastic time-variable rainfall-runoff modelling. In Institute of Engineers Australia National Conference (Vol. 1979, pp. 89-93). Barton, Australia: Institute of Engineers Australia.

IPCC, 2013. Climate Change 2013: *The Physical Science Basis: Summary for Policymakers*. (eds Stocker, T. F. et al.) (Cambridge University Press, Cambridge, 2013).

Melsen, L. A., & Guse, B. (2019). Hydrological drought simulations: How climate and model structure control parameter sensitivity. *Water Resources Research*, 55, 10,527-10547. https://doi.org/10.1029/2019WR025230.

Nadal-Romero, E., Cammeraat, E., Serrano-Muela, M. P., Lana-Renault, N., & Regüés, D. (2016). Hydrological response of an afforested catchment in a Mediterranean humid mountain area: a comparative study with a natural forest. *Hydrological Processes*, 30(15), 2,717-2,733. https://doi.org/10.1002/hyp.10820.

Nie, W., Yuan, Y., Kepner, W., Nash, M. S., Jackson, M., & Erickson, C. (2011). Assessing impacts of Landuse and Landcover changes on hydrology for the upper San Pedro watershed. *Journal of Hydrology*, 407(1-4), 105-114. https://doi.org/10.1016/j.jhydrol.2011.07.012.

Qi, W., Zhang, C., Fu, G., Sweetapple, C., & Zhou, H. (2016). Evaluation of global fine-resolution precipitation products and their uncertainty quantification in ensemble discharge simulations. *Hydrology and Earth System Sciences*, 20(2), 903-920. https://doi.org/10.5194/hess-20-903-2016.

Qi, W., Zhang, C., Fu, G., Zhou, H., & Liu, J. (2016). Quantifying Uncertainties in Extreme Flood Predictions under Climate Change for a Medium-Sized Basin in Northeastern China. *Journal of Hydrometeorology*, 17(12), 3,099-3,112. https://doi.org/10.1175/JHM-D-15-0212.1.

Schilling, K. E., Gassman, P. W., Kling, C. L., Campbell, T., Jha, M. K., Wolter, C. F. & Arnold, J. G. (2014). The potential for agricultural land use change to reduce flood risk in a large watershed. *Hydrological Processes*, 28(8), 3,314-3,325. https://doi.org/10.1002/hyp.9865.

Silvestro F, Rebora N, Ferraris L. Quantitative flood forecasting on small-and medium-sized basins: a probabilistic approach for operational purposes[J]. Journal of Hydrometeorology, 2011, 12(6): 1432-1446.

Song, S., Xu, Y. P., Wu, Z. F., Deng, X. J., & Wang, Q. (2019). The relative impact of urbanization and precipitation on long-term water level variations in the Yangtze River Delta. Science of the Total Environment, 648, 460-471. https://doi.org/10.1016/j.scitotenv.2018.07.433.

Tang, Q., Zhang, X., Duan, Q., Huang, S., Yuan, X., Cui, H., Li, Z. & Liu, X. (2016). Hydrological monitoring and seasonal forecasting: *Progress and perspectives. Journal of Geographical Sciences*, 26 (7), 904-920. https://doi.org/10.1007/s11442-016-1306-z.

Wang, Q., Xu, Y., Wang, Y., Zhang, Y., Xiang, J., Xu, Y., & Wang, J. (2020). Individual and combined impacts of future land-use and climate conditions on extreme hydrological events in a representative basin of the Yangtze River Delta, China. *Atmospheric Research*, 236, 104805. https://doi.org/10.1016/j.atmosres.2019.104805.

Wang, Q., Xu, Y., Xu, Y., Wu, L., Wang, Y., & Han, L. (2018). Spatial hydrological responses to land use and land cover changes in a typical catchment of the Yangtze River Delta region. *CATENA*, 170, 305-315. https://doi.org/10.1016/j.catena.2018.06.022.

Wang Q., Xu Y., Wang Y., Wang J., Zhou C. Y., Fu W., Zhao Y. (2019). Comparative experimental observations and hydrological response in representative basins of Eastern China. *Advances in Water Science*, 30(4), 467-476. DOI: 10.14042/j.cnki.32.1309.2019.04.002.

Wang, Y., Xu, Y. P., Lei, C., Li, G., Han, L., Song, S., Yang, L. & Deng, X. (2016). Spatio-temporal characteristics of precipitation and dryness/wetness in Yangtze River Delta, eastern China, during 1960–2012. *Atmospheric Research*, 172, 196-205. https://doi.org/10.1016/j.atmosres.2016.01.008.

Winsemius, H. C., Aerts, J. C. J. H., Van Beek, L. P. H., Bierkens, M. F. P., Bouwman, A., Jongman, B., et al. (2016). Global drivers of future river flood risk. *Nature Climate Change*, 6(4), 381-385. https://doi.org/10.1038/nclimate2893.

Woldesenbet, T. A., Elagib, N. A., Ribbe, L., & Heinrich, J. (2017). Hydrological responses to land use/cover changes in the source region of the Upper Blue Nile Basin, Ethiopia. *Science of the Total Environment*, 575, 724-741. https://doi.org/10.1016/j.scitotenv.2016.09.124.

Yan, B., Fang, N. F., Zhang, P. C., & Shi, Z. H. (2013). Impacts of land use change on watershed streamflow and sediment yield: An assessment using hydrologic modelling and partial least squares regression. *Journal of Hydrology*, 484(6), 26-37. https://doi.org/10.1016/j.jhydrol.2013.01.008.

Yang, L., Smith, J. A., Baeck, M. L., & Zhang, Y. (2016). Flash flooding in small urban watersheds: Storm event hydrologic response. *Water Resources Research*, 52(6), 4,571-4,589. https://doi.org/10.1002/2015WR018326.

Yang, L., Smith, J., Baeck, M. L., Smith, B., Tian, F., & Niyogi, D. (2016). Structure and evolution of flash flood producing storms in a small urban watershed. *Journal of Geophysical Research: Atmospheres*, 121(7), 3,139-3,152. https://doi.org/10.1002/2015JD024478.

Yang, L., Wang, L., Li, X., Gao, J. (2019). On the flood peak distributions over China, Hydrology and Earth System Sciences, 23, 5133–5149, 2019.

Yin, J., Gentine, P., Zhou, S., Sullivan, S. C., Wang, R., Zhang, Y., & Guo, S. (2018). Large increase in global storm runoff extremes driven by climate and anthropogenic changes. *Nature Communications*, 9 (1), 1-10. https://doi.org/10.1038/s41467-018-06765-2.

Zhou, F., Xu, Y., Chen, Y., Xu, C. Y., Gao, Y., & Du, J. (2013). Hydrological response to urbanization at different spatio-temporal scales simulated by coupling of CLUE-S and the SWAT model in the Yangtze River Delta region. *Journal of Hydrology*, 485, 113-125. https://doi.org/10.1016/j.jhydrol.2012.12.040.

Zhou, Z., Smith, J. A., Yang, L., Baeck, M. L., Chaney, M., Ten Veldhuis, M., et al. (2017). The complexities of urban flood response: Flood frequency analyses for the Charlotte metropolitan region. *Water Resources Research*, 53(8), 7,401-7,425. https://doi.org/10.1002/2016WR019997.

Zhuang, D. & Liu J. (1997). study on the model of regional differentiation of land use degree in china. *J. Nat. Resour*. 2, 105–111.

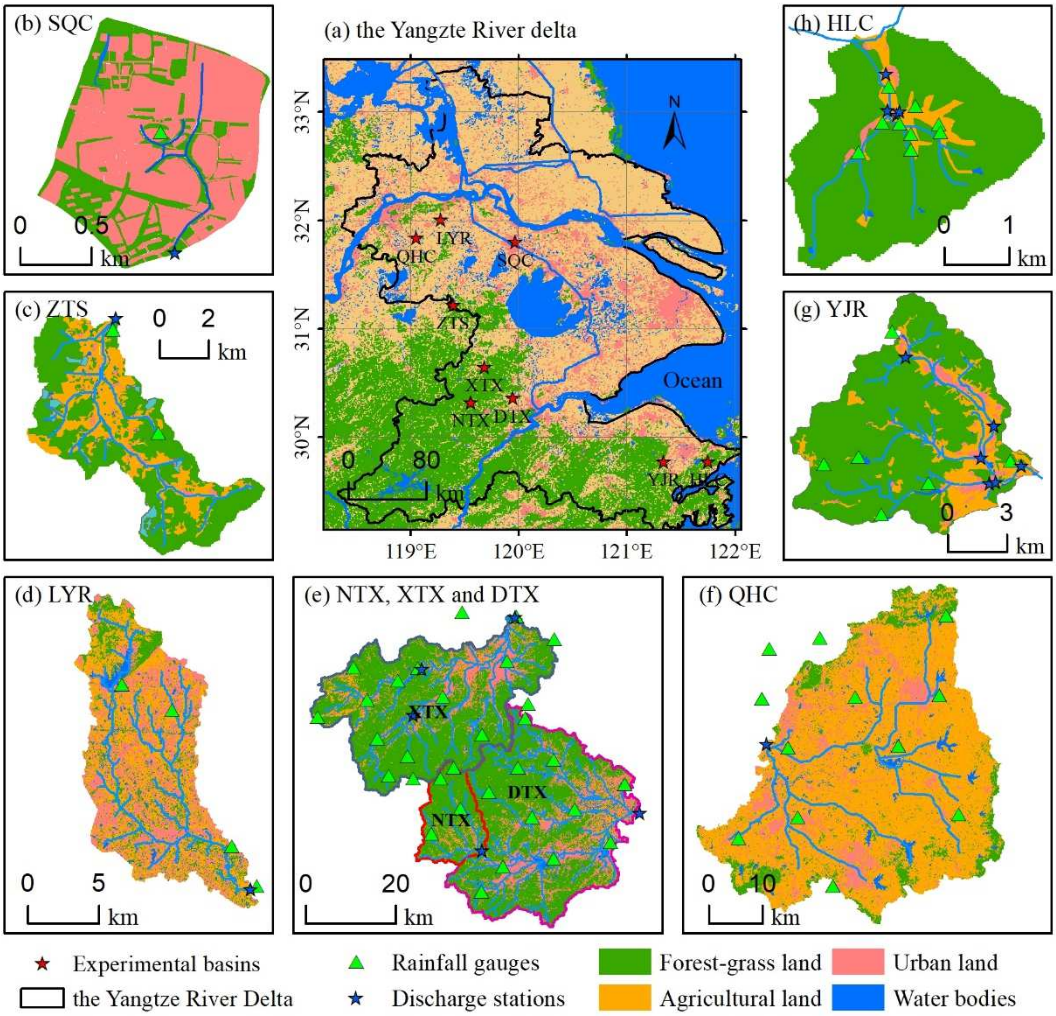

Figure 1. (a) Locations of the Yangtze River Delta region and the experimental basins; (b-h) The land use and land cover maps of the study area in 2015.

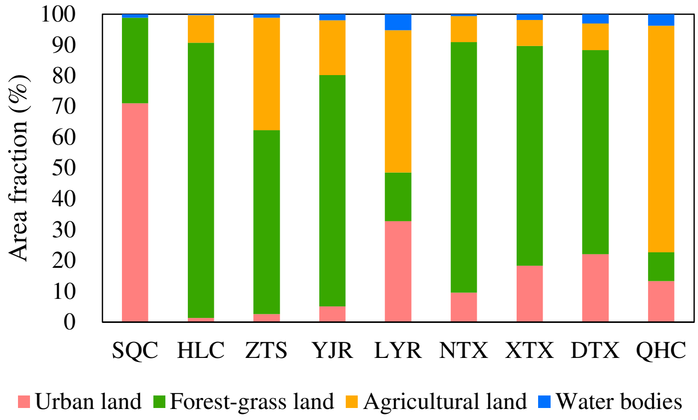

Figure 2. The land use and land cover structures of each watershed in 2015.

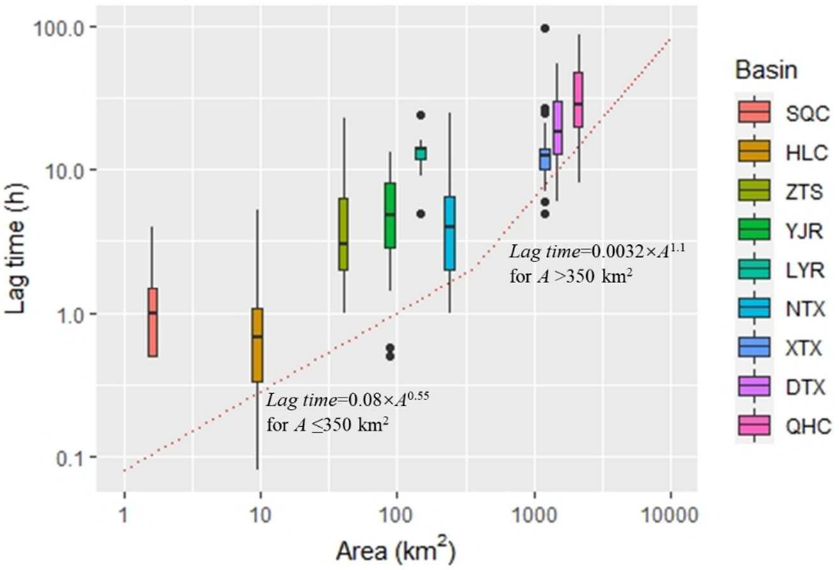

Figure 3. Flood lag time versus drainage area for the observed watersheds. The upper and lower ends of the box represent the 25th and 75th percentiles, respectively, while the line inside the box represents median values. The whiskers of each boxplot extend to one and a half times the interquartile range. The outliers are plotted using the black points. The envelope dotted red lines and equations describe the bottom limit of the lag time (h) versus washed area (A, km^2) from Creutin et al. (2013).

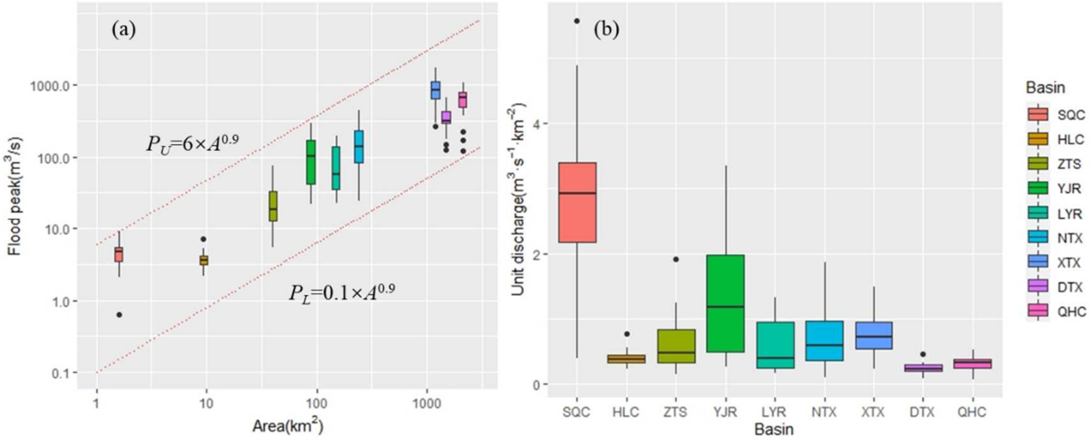

Figure 4. Box plot of flood peak and unit discharge flood peak. The upper and lower sides of the box represent the 25th and 75th percentiles, while the line inside represent the median values. The whiskers of each boxplot extend to one and a half times the interquartile range. The outliers are plotted using the black points. The envelope red dotted lines and the equations mark the bottom (P_L, h) and upper (P_U, h) limit of peak discharge for floods, respectively, and A (km^2) represents the watershed area.

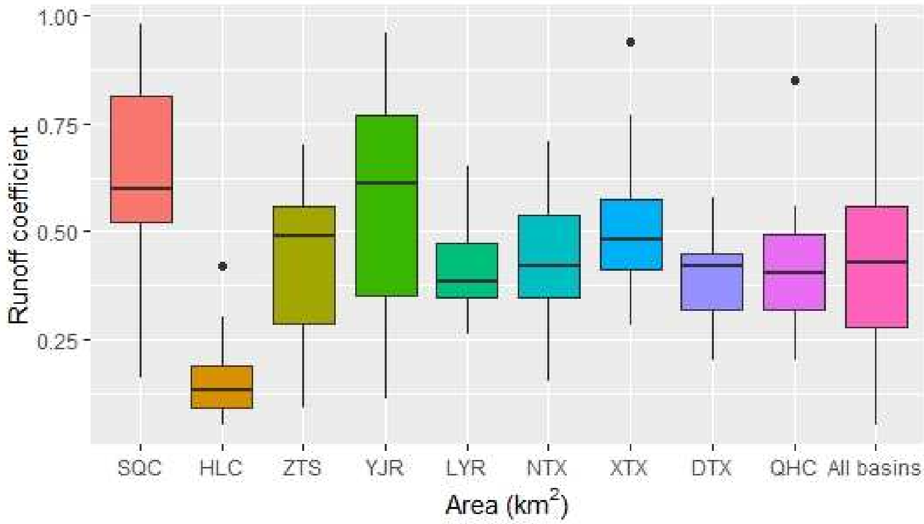

Figure 5. The distribution of runoff coefficient of the studied watershed. The upper and lower edges of the box represent the 25th and 75th percentiles, respectively, while the lines inside represent the median values. The whiskers of each boxplot extend to one and a half times the interquartile range. The outliers are plotted using black points.

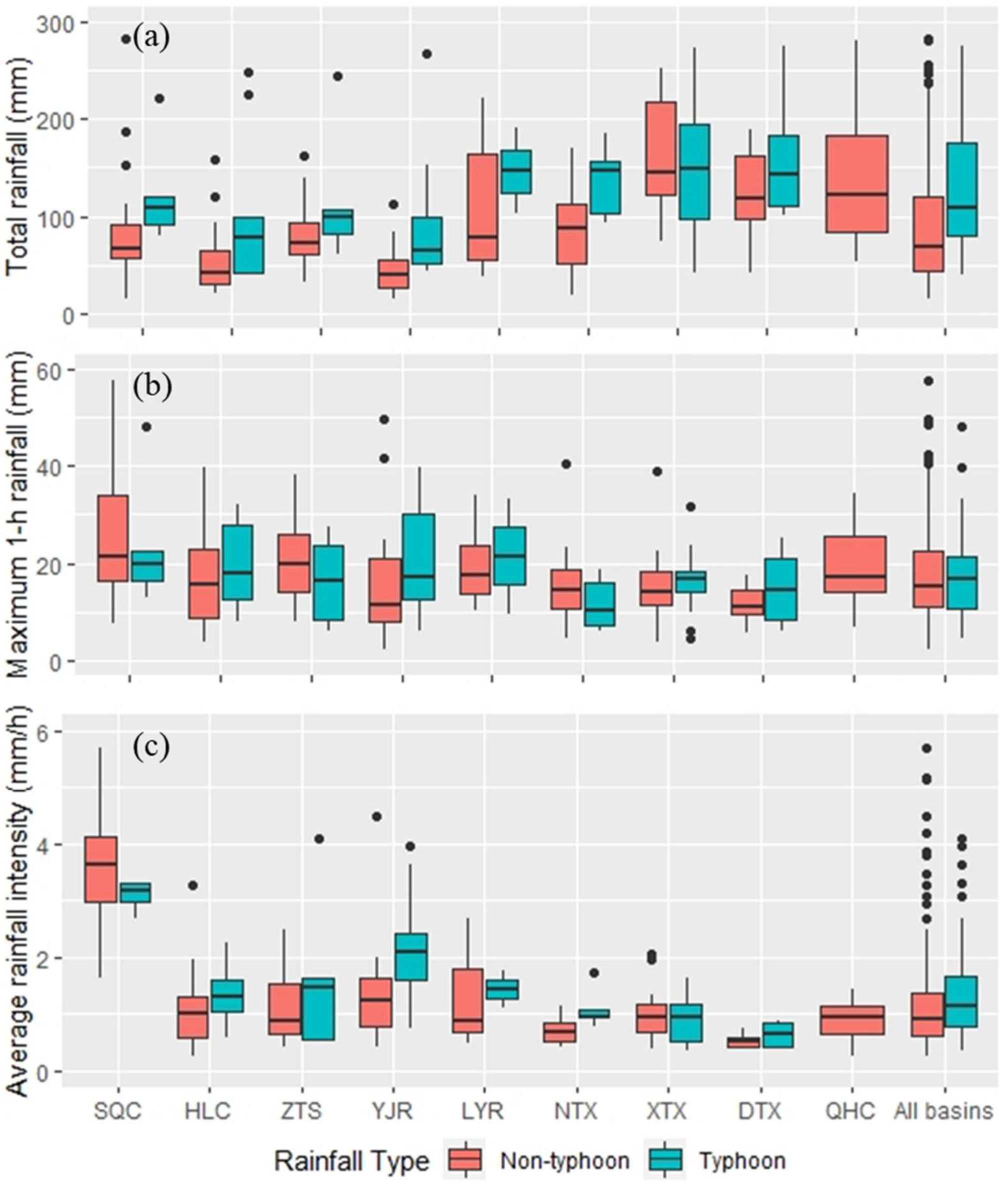

Figure 6. The rainstorm characteristics under typhoon and other weather systems. The upper and lower edges of the box represent the 25th and 75th percentiles, respectively, while the lines inside represent the median values. The whiskers of each boxplot extend to one and a half times the interquartile range. The outliers are plotted using black points.

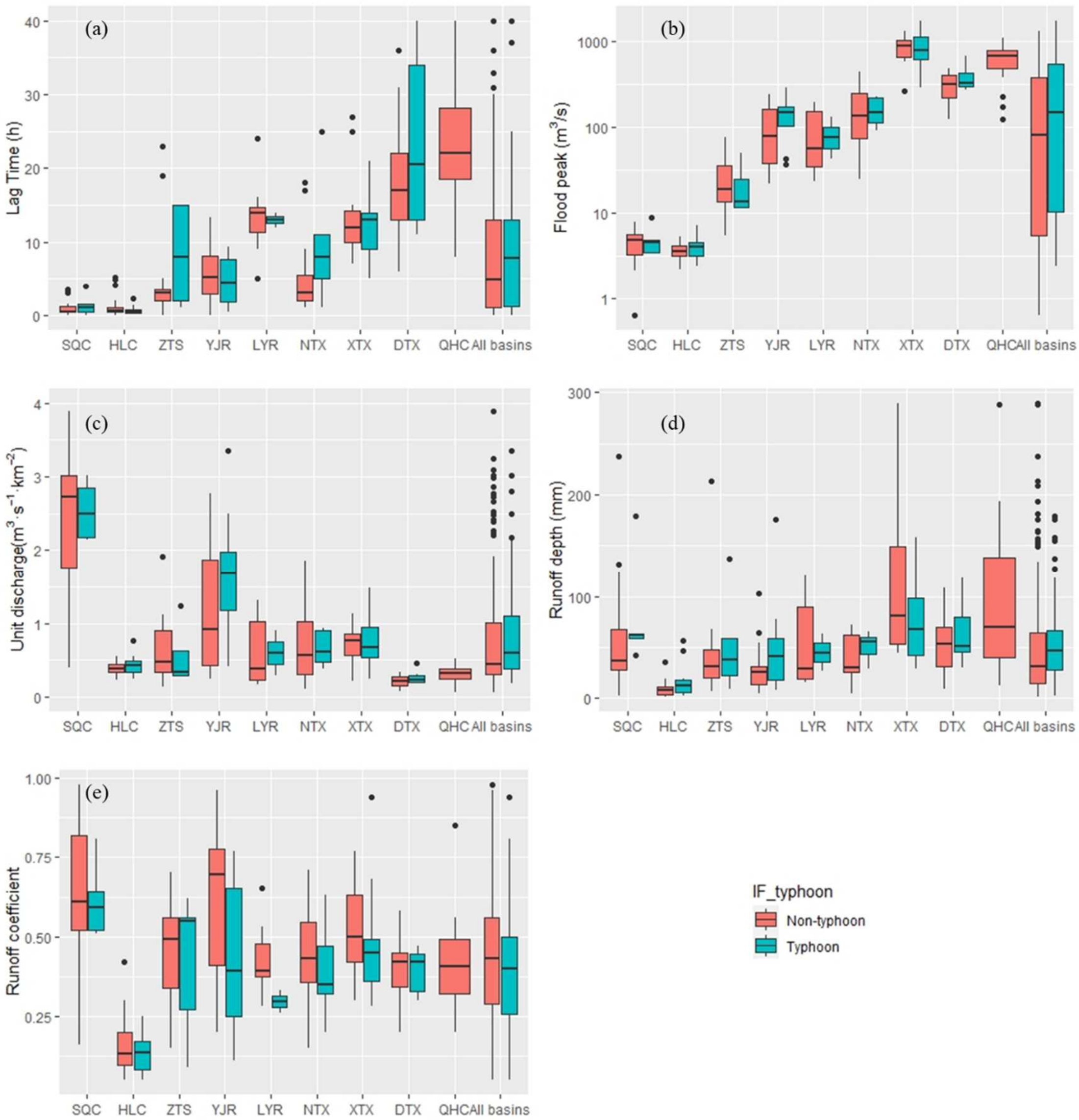

Figure 7. The distribution of flood characteristics under typhoon and without typhoon. The upper and lower edges of the box represent the 25th and 75th percentiles, respectively, while the lines inside represent the median values. The whiskers of each boxplot extend to one and a half times the interquartile range. The outliers are plotted using black points.

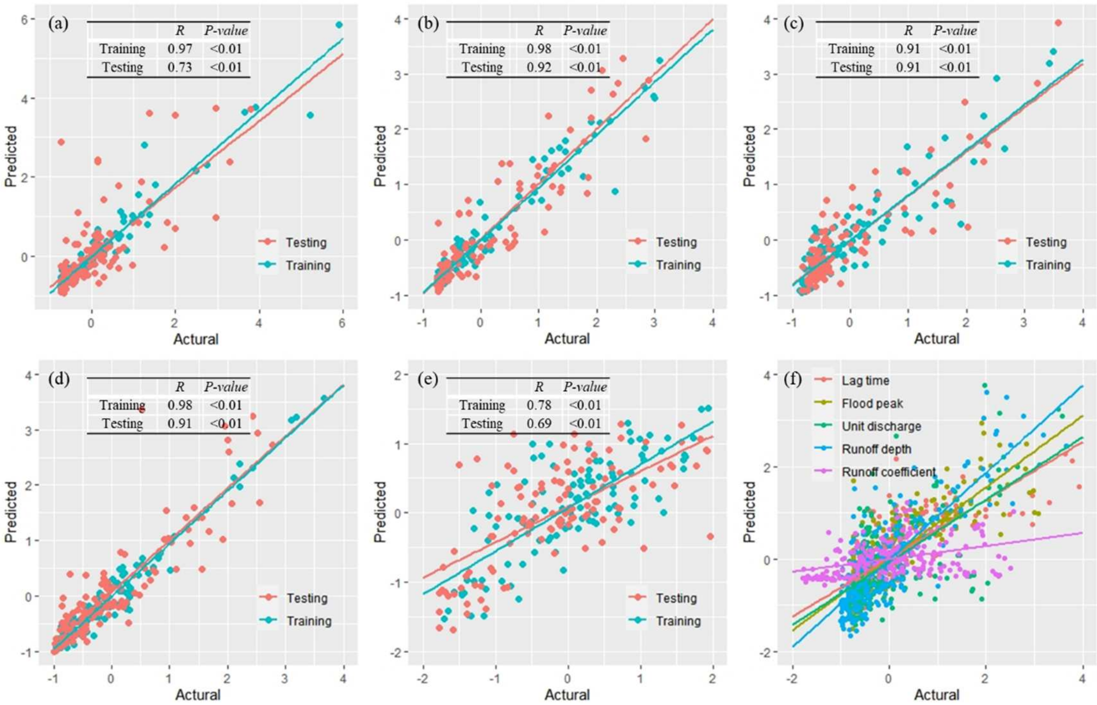

Figure 8. Model predictions versus actual flood lag time (a), flood peak (b), unit discharge (c), runoff depth (d), and runoff coefficient (e) using ANN method, respectively. (f) The fitting result of predictions and observations of each flood characteristics using PCR method, with all significant (p<0.01).

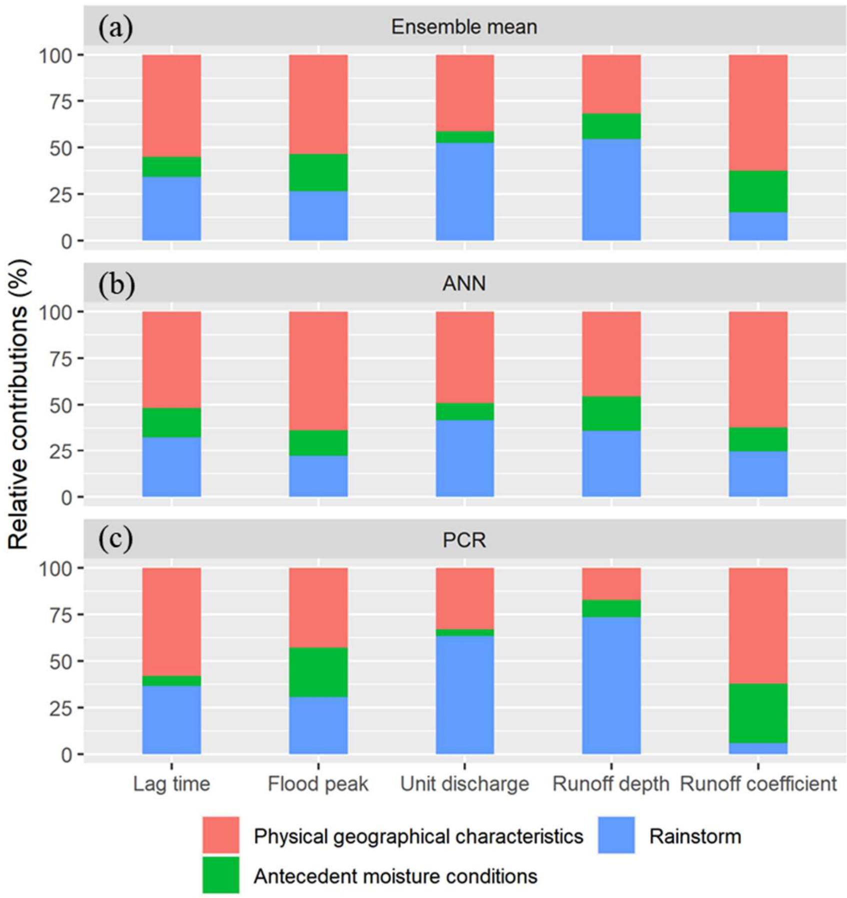

Figure 9. The relative contributions of each influential factor to each flood characteristic estimated by ANN, PCR and ensemble mean.

Table 1. The observed representative basins in the Yangtze River Delta region and the physiographic characteristics of each basin in 2015

Watershed name	Abbreviation	Area (km^2)	Impervious (%)	Land use intensity	River length (km)	River density (km/km^2)	Slope (%)	Spatial Scale	Urbanization level
Shuangqiao Catchment	SQC	1.6	93.41	340.74	1.65	1.02	5.2	Small	High
Hualong Creek	HLC	9.4	0.13	211.12	11.38	1.21	26.8	Small	Low
ZhongTianShe River	ZTS	40.0	0.63	240.31	38.53	0.96	19.3	Small	Low
Yinjiang-Jiaokou River	YJR	88.0	3.95	225.83	58.31	0.65	31.0	Small	Low
Luoyang River	LYR	149.4	9.63	306.38	106.63	0.73	7.1	Small	Medium
Nantiaoxi Basin	NTX	240.7	0.76	226.71	90.72	0.38	8.6	Small	Medium
Xitiaoxi River	XTX	1191.5	7.98	223.96	436.37	0.35	34.9	Medium	Medium
Dongtiaoxi River Basin	DTX	1489.1	8.48	249.54	688.90	0.46	22.8	Medium	Medium
Qianhancun Basin	QHC	2106.7	14.82	282.68	253.11	0.12	11.1	Medium	Medium

Table 2. The numbers of rain gauges, discharge station, and observed flood events during the rainy season (Apr-Oct) for each watershed

Watersheds	Rainfall gauges	Discharge stations	Time periods	Rainstorm flood events		
				Typhoon	Non-Typhoon	Total
SQC	1	1	2015-2018	5	19	24
HLC	9	1	2015-2018	10	31	41
ZTS	2	1	2015-2018	5	15	20
YJR	6	1	2015-2018	9	28	37
LYR	5	1	2015-2018	2	10	12
NTX	6	1	2013-2017	5	19	24
XTX	12	1	1990-2017	17	17	34
DTX	14	1	2013-2017	6	14	20
QHC	10	1	1990-2017	0	28	28
Total	65	9	-	59	181	240

Table 3. The Pearson correlation coefficient (R) of floods with respect to rainstorm characteristics

Flood characteristics	Rainstorm characteristics	SQC	HLC	ZTS	YJR	LYR	NTX	XTX	DTX	QHC
Flood peak	Total rainfall	0.63**	0.73**	0.63**	0.49**	0.89**	0.51*	0.60**	0.86**	0.59**
	Average rainfall intensity	0.67**	0.60**	0.39	0.39*	0.87**	0.40	0.50**	0.69**	0.44*
	Maximum 1-h rainfall	0.71**	0.68**	0.54*	0.26	0.80**	0.46*	0.52**	0.37	0.51**
Unit discharge	Total rainfall	0.74**	0.80**	0.78**	0.50**	0.90**	0.41*	0.63**	0.90**	0.67**
	Average rainfall intensity	0.78**	0.62**	0.41	0.37*	0.85**	0.44*	0.45**	0.76**	0.41*
	Maximum 1-h rainfall	0.82**	0.76**	0.47	-0.21	0.72**	0.47*	0.46**	0.50*	0.55**
Runoff depth	Total rainfall	0.98**	0.80**	0.94**	0.81**	0.94**	0.78**	0.93**	0.94**	0.95**
	Average rainfall intensity	0.44*	0.28	0.32	0.46**	0.77**	0.37	0.33	0.61**	0.17
	Maximum 1-h rainfall	0.41*	0.49**	0.32	0.36*	0.58*	-0.03	0.17	0.29	0.54**
Runoff coefficient	Total rainfall	0.30	0.05	0.14	-0.16	0.65*	0.05	0.09	0.57**	0.16
	Average rainfall intensity	0.09	-0.29	-0.20	-0.42**	0.72**	0.01	-0.12	0.33	-0.05
	Maximum 1-h rainfall	-0.08	-0.17	-0.14	-0.35*	0.38	0.06	-0.17	-0.08	0.17

Note. ** are for $p<0.01$, and * are for $p<0.05$.

Table 4. The Pearson correlation coefficients between each flood characteristic and antecedent watershed conditions

Flood characteristics	Antecedent conditions	SQC	HLC	ZTS	YJR	LYR	NTX	XTX	DTX	QHC
Flood peak	Initial discharge	0.16	0.40**	0.21	0.06	0.23	0.16	0.02	-0.03	0.40*
	Antecedent wetness	-0.12	0.02	0.03	-0.06	0.20	0.32	-0.02	0.03	-0.08
Unit discharge	Initial discharge	0.11	0.34*	0.14	-0.00	0.20	0.12	-0.03	-0.05	0.52**
	Antecedent wetness	-0.21	0.00	0.02	-0.06	0.18	0.21	-0.10	-0.03	-0.18
Runoff depth	Initial discharge	-0.02	-0.22	-0.05	-0.01	-0.14	0.07	0.03	-0.08	0.46*
	Antecedent wetness	-0.17	-0.12	-0.05	-0.04	-0.15	0.20	-0.17	-0.08	-0.38*
Runoff coefficient	Initial discharge	0.03	-0.34*	-0.11	0.35*	-0.02	0.09	0.29	0.01	0.28
	Antecedent wetness	0.40*	-0.14	-0.13	0.00	-0.02	0.21	0.19	0.12	0.03

Note. ** are for $p<0.01$, and * are for $p<0.05$.

Graphical abstract

The multi-scale observed watersheds in the Yangtze River Delta

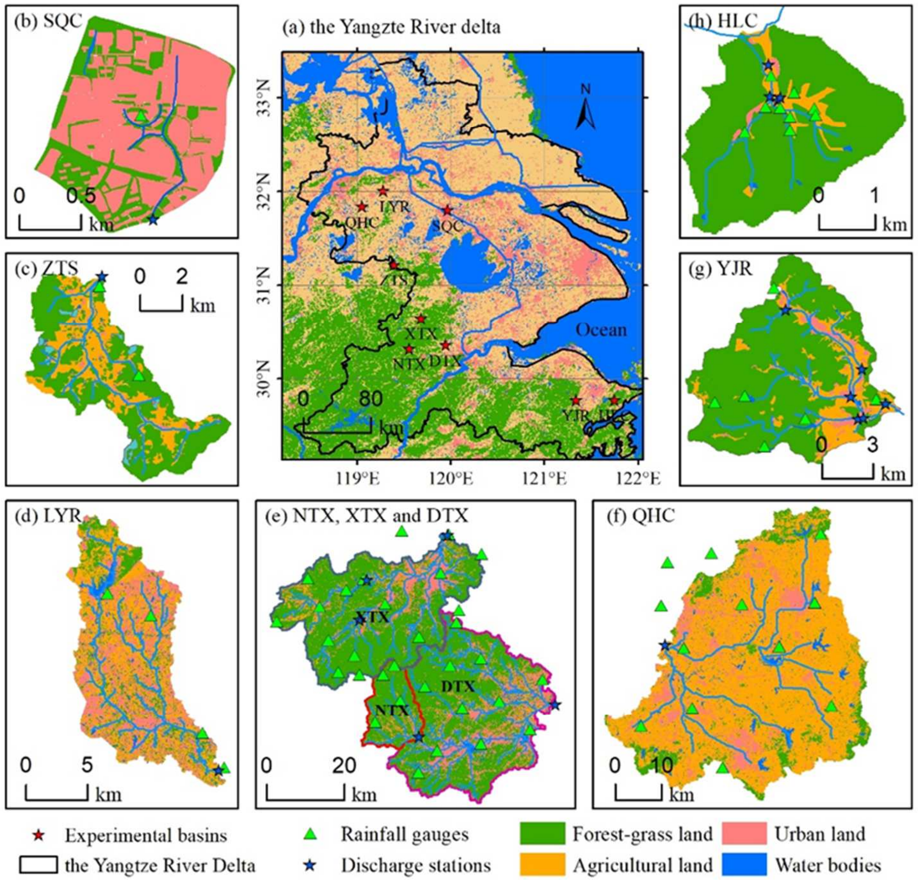

The relative contributions of influencing factors to flood characteristics